J Physiol Sci (2009) 59:299–305
DOI 10.1007/s12576-009-0036-8

ORIGINAL PAPER

# Typical dipole locations can be estimated using averaged somatosensory-evoked potentials and a standard brain model

**Yuri Masaoka · Hiroyoshi Yajima · Miho Takayama · Akiko Kawase · Nobuari Takakura · Ikuo Homma**

Received: 25 February 2009 / Accepted: 16 March 2009 / Published online: 8 April 2009
© The Physiological Society of Japan and Springer 2009

**Abstract** It is reasonable to hypothesize that dipoles estimated from grand averaged event-related potentials based on summed-up data obtained from multiple subjects and standard head models could correspond to typical brain regions associated to a particular event. Six healthy subjects were enrolled in a study to test this hypothesis. We estimated dipoles from somatosensory-evoked potentials (SEP) elicited by electrical stimulation to the left median nerve. We also created individual three-layered (scalp, skull, and brain) head models from each subject's magnetic resonance imaging scan, and dipoles were estimated from the individual averaged SEP with each individual head model. We then estimated dipoles using grand averaged SEP across all subjects on the standard head model created from the Montreal Neurological Institute (MNI) standard coordinate system brain template to compare the estimated dipoles located on our own head model and those on the MNI. The dipoles in the post-central gyrus were estimated from negative potentials at 20 ms from the grand averaged data incorporated with the MNI head model, corresponding to a typical location related to SEP stimulation. The results suggest the validity of estimating the dipole location from the grand averaged potential of all subjects with the MNI model if we focus on typical regions related to the task.

**Keywords** Dipole estimation · Grand averaged potentials · Individual head model · Montreal Neurological Institute · Somatosensory-evoked potentials

Y. Masaoka · H. Yajima · M. Takayama · A. Kawase · N. Takakura
The Educational Foundation of Hanada Gakuen, Department of Acupuncture and Moxibustion, Faculty of Health Sciences, Tokyo Ariake University of Medical and Health Sciences, 2-9-1 Ariake, Koto-ku, Tokyo 135-0063, Japan

Y. Masaoka · H. Yajima · M. Takayama · A. Kawase · N. Takakura · I. Homma (✉)
Department of Physiology II, Showa University School of Medicine, 1-5-8 Hatanodai, Shinagawa-ku, Tokyo 142-8555, Japan
e-mail: ihomma@med.showa-u.ac.jp

H. Yajima · M. Takayama · A. Kawase · N. Takakura · I. Homma
The Foundation for Oriental Medicine Research, 28-9 Sakuragaoka-Machi, Shibuya-ku, Tokyo 150-0031, Japan

## Introduction

Electroencephalograph (EEG) dipole fitting has been developed to localize dipoles estimated from event-related potentials (ERP) in the brain model and to visualize the point-like dipole in the anatomical brain regions. Dipole analysis can be performed for visual [1, 2], olfactory [3], and movement-related potentials [4] as well as on raw data obtained from the interictal spike in patients with epilepsy [5]. An advantage of dipole fitting is that it enables the researcher to locate the dipole in millisecond intervals, thereby allowing the dipole's movement to be observed and, consequently, the process of brain activation to be detected. Dipole results can be superimposed on magnetic resonance imaging (MRI) scans in order to identify the anatomical regions associated with the sensory events. Although the dipole fitting model has a great potential for human brain mapping, it seems to be difficult to use in routine experiments and clinical examinations, possible due to the two factors. (1) It is not always possible to use MRI (slice from brainstem to vertex) to construct a subject's own head model, and although a spherical model can

be used, it is hard to find an accurate dipole location in such a model. (2) An EEG is greatly affected by background noise. It is therefore necessary to obtain the average from a number of trials to increase the signal to noise (S/N) ratio to estimate accurate dipole localization. Scattered dipole localizations are attributed to a low S/N ratio, which makes it difficult to identify significant localization related to the event. However, a large number of trials on one subject increases the S/N ratio, causing subjects to become tired and adapted toward stimuli.

As a means to counter these problems, we hypothesized that dipole locations estimated from grand averaged event-related potentials based on summed-up data obtained from multiple subjects with a standard head model could correspond to a typical region related to stimuli. To test this hypothesis, we performed experiments using the following procedures. (1) Dipole locations were estimated from the grand averaged somatosensory-evoked potentials (SEPs) from all the subjects incorporated with the standard head model created from the Montreal Neurological Institute (MNI) brain template, which serves as the most common stereotaxic platform [6]. (2) We also created an individual three-layer (scalp, skull, and brain) head model from each subject's MRI scan. Dipoles were estimated from the individual averaged SEPs with the individual head model. (3) We confirmed that the dipole locations estimated from grand averaged potentials with the MNI brain head model corresponded to specific brain areas that had been already identified by neuroimaging studies. We also compared the difference between dipole localization of grand averaged potentials across subjects with the standard MNI model and the dipole localization of averaged potentials within subjects with the individual head model. We investigated whether dipole estimation from grand averaged potentials with the MNI brain head model is a reliable procedure by which to determine the typical regions associated with the stimuli.

## Method

The study cohort consisted of six healthy subjects (mean age 38.3 ± 13.3 years). All subjects signed an informed consent, and the study protocol was approved by the Ethics Committee of Showa University School of Medicine.

### Measurement of EEG and SEP

Subjects lay on a couch in a shielded room, with their eyes closed. The subject's head was supported with a pillow to avoid unnecessary muscle tension. Nineteen electrodes were arranged according to the 10–20 system, with the reference electrode attached to the right earlobe. Electro-oculograms (EOG) were recorded with the electrodes placed at the inferior lateral cantus and supraorbitally to the left eye. Electrode impedances were held below 5 kΩ throughout the EEG recording. Potentials were measured by an EEG recorder (EEG-1100; Nihon Kohden, Tokyo) at 1000-Hz intervals and stored on magnetic optical disks for off-line analysis. Potentials were digitally filtered by a band pass-filtered (5–100 Hz).

A 100-μs rectangular pulse wave was applied by a stimulator (SEN-3301; Nihon Kohden, Tokyo) through electrodes mounted on the skin over the left median nerve at the wrist. The negative electrode was placed on the crease across the anterior surface of the wrist, and the positive electrode was 2 cm distal to the negative electrode. The intensity of stimulation was adjusted to 10–15% over the individual motor threshold and delivered at intervals of 1000 ms. Between 300 and 400 [mean ± standard deviation (SD) 357 ± 53] stimuli were delivered to each subject, and artifacts from eyes and body movements were omitted for averaging. Potentials from 50-ms pre- and 200-ms post-stimuli were averaged.

### Individual head model and MNI standard head model

The procedure for creating the head model and dipole estimation is shown in Fig. 1.

For all subjects, T1 weighted images were taken from the spinal cord to the vertex at a slice thickness of 2 mm. From individual MRIs and MNI images, brain, skull, scalp surfaces were extracted from each slice using Mimics software (Materialise: http://www.materialise.com), and each surface was reconstructed as a polyhedron consisting of 960 triangles. Nineteen electrodes were arranged according to the standard 10–20 method determined by anatomical landmarks (nasion, inion, the right and the left tragus of auricula, and the vertex). Before the dipole was calculated, we calculated the conductivities of the electrodes for the brain (0.3300 s/m), skull (0.0041 s/m), and scalp (0.3300 s/m). A detailed description of the scalp-skull-brain/dipole tracing (SSB/DT) method [Brain Space Navigator (BS-navi); Brain Research and Development, Japan] has been reported elsewhere [2–5, 7]. Dipole results estimated with the individual head model were expressed as coordinates of the MNI head model and superimposed on the MNI brain. Translation from the coordinates of the individual head model to those of the MNI brain head model was determined by the electrodes' positions [4].

## Results

The latency of SEP measured from six subjects and that of SEP measured from grand averaged SEPs indicate that the components are similar (Table 1).

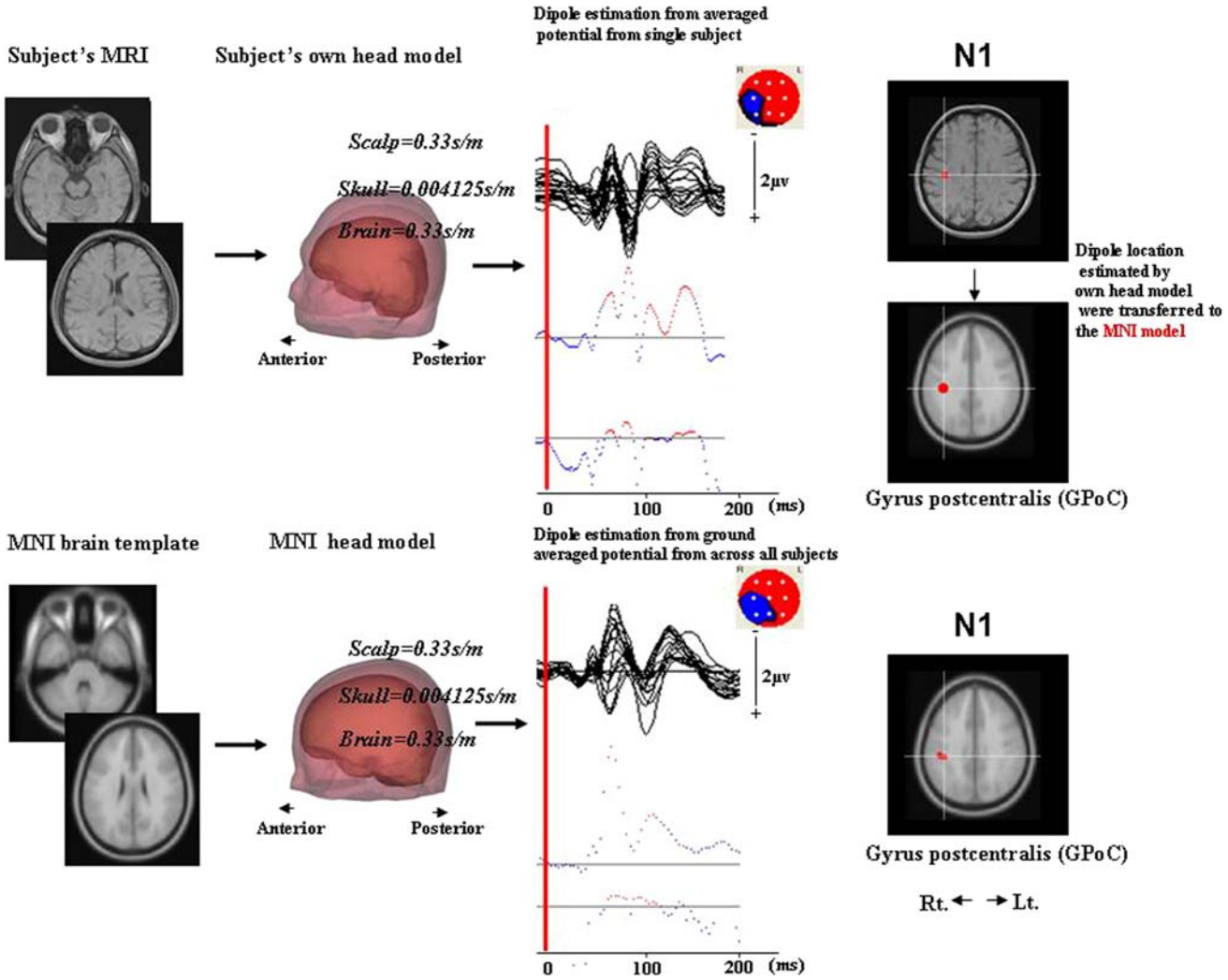


**Fig. 1** *Upper panel* The outlines of the brain, skull, and scalp are extracted from each magnetic resonance imaging (*MRI*) slice (slice thickness 2 mm) and saved as *x*, *y*, and *z* coordinates. Three-layered (scalp, skull, and brain) head models are then reconstructed from the *x*, *y*, and *z* coordinates. Conductivities of the electrodes for the brain (0.3300 s/m), skull (0.0041 s/m), and scalp (0.3300 s/m) are then calculated before the dipole is calculated. Somatosensory-evoked potentials (SEPs) elicited by electrical stimulation to the left median nerve are measured in a subject. Dipole analysis is performed from an individual subject's SEP with his/her own head model, and these dipole locations are superimposed on the Montreal Neurological Institute (*MNI*) head model. *Lower panel* Outlines of the brain, skull, and scalp are extracted from slices of the standard MNI template, and a three-layered head model is reconstructed from the coordinates obtained from each slice. Conductivities are also taken into account for the dipole calculations. All SEPs of all subject are averaged, and dipole analysis is performed from this grand averaged SEP with the MNI model. *Rt* right, *Lt* left

**Table 1** Latencies of SEP components of six subjects and grand averaged potentials

| | N1 | P2 | N2 | P3 | N3 | P4 |
|---|---|---|---|---|---|---|
| Mean ± SD of six subjects | 22 ± 4 | 32.8 ± 6 | 43.8 ± 7.1 | 53.6 ± 7.6 | 67.8 ± 9.5 | 96.6 ± 2.9 |
| Grand averaged SEP | 22 | 30 | 40 | 50 | 62 | 100 |

*SD* standard deviation, *SEP* somatosensory-evoked potential

Figure 2 shows the dipole results in order of SEP component analyzed with the individual head models. Dipoles were superimposed on the correct coordinates of the individual MRI slices. Figure 3 shows the results of dipole localization of Fig. 2 expressed on the MNI image and the results of dipole localization obtained from the grand averaged potentials from all subjects calculated with the MNI brain model. The *x*, *y*, and *z* coordinates of dipole locations are shown above each MNI slice, and anatomical regions were confirmed using the Talairach

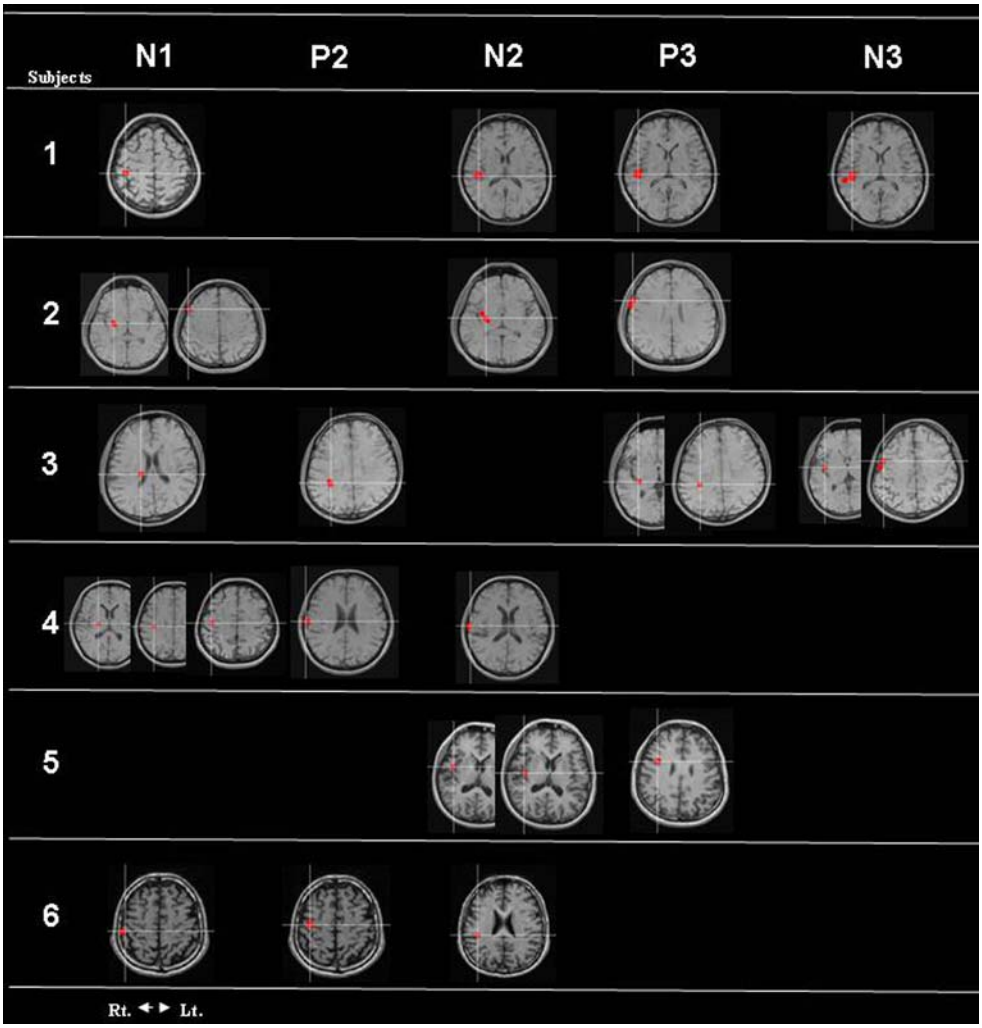


**Fig. 2** Dipole locations estimated from individual SEPs with individual head models. The results from six subjects are shown in order of the SEP component: N1, P2, N2, P3, and N3. *Rt* right, *Lt* left

Brain Atlas [8], which are indicated at the bottom of each MNI slice.

In Figure 3, in the N1 component, dipoles were located in the gyrus precentralis (GPrC), gyrus postcentralis (GPoC), and sulcus centralis cerebri (SC). Dipoles were also found in the fasciculus longitudinalis superior (FLS), the nucleus caudatus (NC), and the thalamus (TH). At P2, three of six subjects' dipoles were not estimated. For three subjects, each estimated dipole was in the GPrC, GPoC, or SC. In the N2 component, dipole localization varied from subject to subject: in the GPrC, GPoC, the insula (INS), the radiatio acustica (RA), the putamen (Pu), and the sulcus lateralis cerebri (SI). At P3, dipoles were observed in the SC, GPrC, INS, and FLS. There were no estimated dipoles in two subjects. At N3, dipoles were estimated in the GPoC, and GPoC and INS.

Anatomical regions of dipole locations are summarized in Table 2. The number of dipoles estimated from individual averaged potentials with individual head models and from averaged potentials with the MNI head model. The dipole localization estimated from grand averaged potentials across all subjects with the MNI model is in the GPoC at N1 and in the SC at P2 and N2.

## Discussion

### Grand averaged data sets with the MNI model

In this study, we tested the hypothesis that results of dipole localization from grand averaged potentials across all subjects incorporated with a standard MNI head model could show typical regions related to SEP. Dipole locations estimated with the MNI model were also compared with areas estimated from individual averaged potentials incorporated with individual head models.

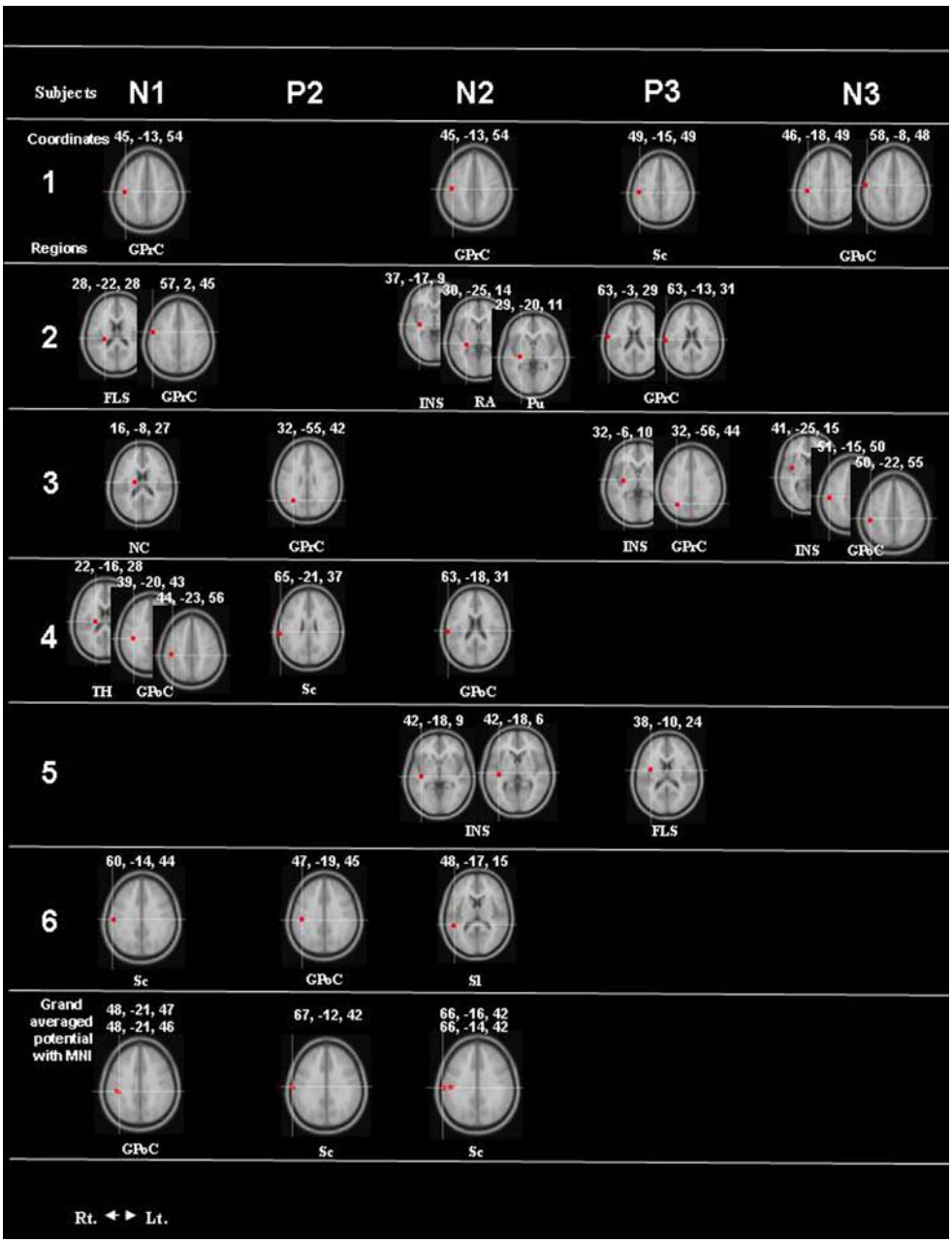


**Fig. 3** Dipole locations estimated in each individual head model were superimposed on the coordinates of the MNI model. The *x*, *y*, and *z* coordinates of dipole locations are indicated *above* each MNI slice, and anatomical regions confirmed by Talairach Brain Atlas are shown at the *bottom* of each MNI slice. *Lower panel* Dipole analysis performed from grand averaged SEP for all subjects with the MNI model is indicated. Anatomical regions: *GPrC* gyrus precentralis, *GPoC* gyrus postcentralis, *FLS* fasciculus longitudinalis superior, *NC* nucleus caudatus, *TH* thalamus, *SC* sulcus centralis cerebri, *RA* radiatio acustica, *PU* putamen, *INS* insula, *SI* sulcus lateralis cerebri. *Rt* right, *Lt* left

We confirmed that dipoles estimated from grand averaged data sets with the MNI head model converged in the GPoC at N1 of SEP (corresponded with N20). This is the primary somatosensory cortex (SI), which has been reported in magnetoencephalography (MEG) and EEG studies [9, 10]. In addition, dipoles estimated from grand averaged data sets with the MNI head model showed more typical locations related to SEP stimuli than those observed in the individual head models. The results of one study suggest that increasing the number of data points to the average enhances the S/N ratio and, consequently, estimations based on averaged potentials with high S/N ratios incorporated with MNI show convergence to typical regions [4]. Whittingstall et al. [11] investigated the difference in dipole location between the individual and grand averaged data sets with a standard realistic head model

**Table 2** Anatomical regions of dipole location

| Anatomical region | N1 | P2 | N2 | P3 | N3 | P4 |
|---|---|---|---|---|---|---|
| GPrC | ○○ | ○ | ○ | ○○ | | |
| GPoC | ○○●● | ○ | ○ | | ○○ | |
| FLS | ○ | | | ○ | | |
| NC | ○ | | | | | |
| TH | ○ | | | | | |
| SC | ○ | ○●● | ●● | ○ | | |
| RA | | | ○ | | | |
| PU | | | ○○ | | | |
| INS | | | ○ | ○ | ○ | |
| SI | | | ○ | | | |

*Open circle* Number of dipoles estimated from individual averaged potential with individual head models, *closed circle* number of dipoles estimated from grand averaged all subjects' potentials with the MNI head model

*GPrC* Gyrus pre centralis, *GPoC* gyrus postcentrals, *FLS* fasciculus longitudinalis superior, *NC* nucleus caudatus, *TH* thalamus, *SC* sulcus centralis cerebri, *RA* radiatio acustica, *PU* putamen, *INS* insula SI sulcus lateralis cerebri

derived from MNI and concluded that a standard head model is useful when the S/N ratio is high. Our results are consistent with those of prior studies showing that the convergence of dipoles in specific areas may be a result of high S/N ratios based on increases in averaging potentials.

Reliable results of dipole estimation can be obtained from individual averaged potentials with the subject's own head model if the S/N ratio is high. However, we speculated that to increase the S/N ratio, a large number of trials would be needed in order to average the data obtained on one subject. In a laboratory situation, especially for clinical patients, a large number of trials could result in patients becoming tired or feeling unpleasant. In addition, it is difficult to measure 2-mm MRI slices from the brainstem to the vertex levels in order to create a head model for each subject/patient. We suggest that dipole estimation from grand averages across all subjects with MNI could be useful when all subjects' head models are not available, when there are data of event-related potentials measured from a number of subjects, and if the focus is on typical regions related to stimuli.

### Area related to SEP

Dipoles in the GPrC or GPoC were estimated from individual averaged potentials with their own head models; however, in the late SEP component, we estimated the non-primary somaotosensory areas in some subjects. After estimating the N2 component, we activated the secondary somatosensory area (SII) and the INS in parallel with the activation of somatosensory areas in subjects 1, 2, 3, and 5.

Jones and Powell [12] reported that SII areas receive inputs from the SI area. Connections between SI and SII are somatotopically organized [13]. The study of dipole analysis shows that the source of negative potential at 60 ms (N60) is localized in the SII area [14]. In this study, we observed the presence of dipoles localized in the SII and INS in some subjects between N2 and N3 (time range from 43.8 ± 7.1 to 67.8 ± 9.5 ms), corresponding to those potentials observed in the priori study. However, activation of the SII and INS areas was not observed in all subjects. Babra et al. [14] reported that N60 latency was largely decreased at a high stimulus rate of the median nerve, and another study showed that the perisylvian cortex is quite sensitive to stimulus intensity [15]. The activation of the SII and INS might be related to the level of cognitive intensity and sensitiveness toward stimuli.

Subjective feelings or emotional level emerging during the stimuli or during the course of trials could influence the results of field potentials and the result of dipole locations. Activations of the amygdala (AMG) and temporal pole were found in subjects showing a high level of anxiety [16], and the level of fear is known to affect the responses of AMG. [2]. These individual traits indicated by brain activations may disappear by averaging all potentials from a number of subjects.

Based on the results of this study, we suggest that combining potentials based on the sum of data obtained from multiple subjects with an MNI model contribute towards an accurate determination of the location of dipoles specifically associated with the event. This method could be useful to compare brain activations between groups of different ages and sex, for traits measured with a psychological test, or by the stage of disease for certain patients.

**Acknowledgments** The authors thank Mr. Seizo Sasaki, MRI technician, for his assistance.

## References

1. Ikeda H, Nishijo H, Miyamoto K, Tamura R, Endo S, Ono T (1998) Generators of visual evoked potentials investigated by dipole tracing in the human occipital cortex. Neuroscience 84(3):723–739. doi:10.1016/S0306-4522(97)00569-1
2. Yoshimura N, Kawamura M, Masaoka Y, Homma I (2005) The amygdala of patients with Parkinson's disease is silent in response to fearful facial expressions. Neuroscience 131:523–534. doi:10.1016/j.neuroscience.2004.09.054
3. Masaoka Y, Koiwa N, Homma I (2005) Inspiratory phase-locked alpha oscillation in human olfaction: source generators estimated by a dipole tracing method. J Physiol 566:979–997. doi:10.1113/jphysiol.2005.086124
4. Inoue M, Masaoka Y, Kawamura M, Okamoto Y, Homma I (2008) Differences in areas of human frontal medial wall activated by left and right motor execution: dipole-tracing analysis of

grand-averaged potentials incorporated with MNI three-layer head model. Neurosci Lett 437:82–87. doi:10.1016/j.neulet.2008.03.082
5. Homma I, Masaoka Y, Hirasawa K, Yamane F, Hori T, Okamoto Y (2001) Comparison of source localization of interictal epileptic spike potentials in patients estimated by the dipole tracing method with the focus directly recorded by the depth electrodes. Neurosci Lett 304:1–4. doi:10.1016/S0304-3940(01)01746-3
6. Brett M, Johnsrude IS, Owen AM (2002) The problem of functional localization in the human brain. Nat Rev Neurosci 3:243–249. doi:10.1038/nrn756
7. Okamoto Y, Homma I (2004) Development of a user-friendly EEG analyzing system specialized for the equivalent dipole method. Int J Bioelectromagn 6:1. Available at: http://www.ijbem.org/volume6/number1/005.htm
8. Talairach J, Tournoux P (1988) Co-planar stereotaxic atlas of the human brain: 3-dimensional proportional system. An approach to cerebral imaging. Thieme Medical, Stuttgart
9. Komssi S, Huttunen J, Aronen HJ, Ilmoniemi RJ (2004) EEG minimum-norm estimation compared with MEG dipole fitting in the localization of somatosensory sources at S1. Clin Neurophysiol 115(3):534–542. doi:10.1016/j.clinph.2003.10.034
10. Urbano A, Babiloni F, Babiloni C, Ambrosini A, Onorati P, Rossini PM (1997) Human short latency cortical responses to somatosensory stimulation. A high resolution EEG study. Neuroreport 8(15):3239–3243
11. Whittingstall K, Stroink G, Gates L, Connolly JF, Finley A (2003) Effects of dipole position, orientation and noise on the accuracy of EEG source localization. Biomed Eng Online 2:14. doi:10.1186/1475-925X-2-14
12. Jones EG, Powell TPS (1969) Connections of the somatic sensory cortex of the rhesus monkey. I. Ipsilateral cortical connections. Brain 92:477–502
13. Manzoni T, Conti F, Fabri M (1986) Callosal projections from area SII to SI in monkeys: anatomical organization and comparison with association projections. J Comp Neurol 252:245–263. doi:10.1002/cne.902520208
14. Barba C, Frot M, Valeriani M, Tonali P, Mauguière F (2002) Distinct fronto-central N60 and supra-sylvian N70 middle-latency components of the median nerve SEPs as assessed by scalp topographic analysis, dipolar source modeling and depth recordings. Clin Neurophysiol 113(7):981–992. doi:10.1016/S1388-2457(02)00104-9
15. Mima T, Ikeda A, Nagamine T, Yazawa S, Kunieda T, Mikuni N, Taki W, Kimura J, Shibasaki H (1997) Human second somatosensory area: subdual and magnetoencefalographic recording of somatosensory evoked responses. J Neurol Neurosurg Psychiatry 63:501–505. doi:10.1136/jnnp.63.4.501
16. Masaoka Y, Homma I (2000) The source generator of respiratory-related anxiety potential in the human brain. Neurosci Lett 283:21–24. doi:10.1016/S0304-3940(00)00895-8